Estimating the Effect of Higher Order Azimuthal Modes in Spherical Near-Field Probe Correction

A.C. Newell, S.F. Gregson
Nearfield Systems Inc.
19730 Magellan Drive,
Torrance, CA 90502-1104
anewell@nearfield.com, sgregson@nearfield.com

Abstract— **The standard numerical analysis used for efficient processing of spherical near-field data requires that the far-field pattern of the probe can be expressed using only azimuthal spherical modes with indices of $\mu = \pm 1$ [1, 2, 3]. In this commonly used approach, the probe is assumed to have only modes for $\mu = \pm 1$, and if the probe has higher order modes, errors will be present within the calculated AUT spherical mode coefficients and the resulting asymptotic far-field parameters. In the event that the probe satisfies this symmetry requirement, then near-field data is only required for two angles of probe rotation about its axis of $\chi = 0$ and 90 degrees and numerical integration in χ is not required. This reduces both measurement and computation time as only two orthogonal tangential near electric field components are sampled and processed. Thus, it is highly desirable to use probes that satisfy the $\mu = \pm 1$ criteria. Circularly symmetric probes can be constructed that reduce the higher order modes to very low levels. Examples of these devices include cylindrical waveguide probes that are excited by the TE_{11} fundamental mode. However for probes using open ended rectangular waveguides (OEWG) the effect of the higher order modes can also be limited by using a measurement radius that reduces the subtended angle of the AUT at the probe.**

Some analysis and simulation have been published that estimate the effect of using a probe with higher order modes [4, 5, 6, 7, 8] and the following study is another effort to develop further guidelines for the properties of the probe and the measurement radius that will reduce the effect of higher order azimuthal modes to acceptable levels. Previous simulation studies [9, 10, 11] have focused primarily on the effect of higher order azimuthal probe modes in rectangular OEWG probes. These showed that for radii of twice the maximum radial extent (MRE) of the test antenna the differences in the near-field, and far-field, are on the order of -50 dB below the peak amplitudes. For larger measurement radii, the differences were found to be below -60 dB. In contrast to the previously published work, this paper presents the results of a similar study in which a broad-band dual ridged horn antenna was used as a near-field probe for spherical testing. Such probes are often utilized for spherical near-field testing as they have wide frequency bandwidths that cover several, typically three or more, rectangular or circular waveguide bands. Thus, the use of such devices is attractive as they can greatly simplify measurement setup, and minimize test times. Thus, although it does not satisfy the $\mu = \pm 1$ criteria, these probes are widely used within the antenna measurement community. However, comparatively little information is available within the published open literature regarding specific guidelines for the properties of the probe and the measurement radius needed that will reduce the effect of higher order azimuthal modes to acceptable levels and is the motivation for this work. The results of these additional simulations are presented and guidelines developed to aid in the choice of spherical near-field probes and measurement radii for typical antennas are presented and discussed.

Index Terms— **near-field, measurements, near-field probe, spherical, spherical mode analysis.**

I. INTRODUCTION

This paper extends previous simulation studies [9, 10, 11] into the effect of higher order azimuthal probe modes when the classical spherical numerical software which uses the orthogonality approach to solve for the spherical modes of the antenna under test (AUT) is employed. In this commonly used approach, the probe is assumed to have only modes for which $\mu = \pm 1$ with all higher order azimuthal spherical mode coefficients being assumed to be identically zero. In the event the probe has higher order azimuthal modes, as if often the case in practice, errors will be present within the calculated AUT spherical coefficients and the corresponding far-field data. In the previous studies, a computational electromagnetic simulation was developed to calculate the output response for an arbitrary AUT/probe combination where the probe is placed at arbitrary locations on the measurement sphere. The planar transmission equation was used to calculate the probe response using the plane wave spectra for actual AUTs and probes derived from either planar or spherical near-field measurements. The planar transmission formula was utilized as there is no limitation on the characteristics of the AUT or probe thereby enabling an entirely general model to be constructed. The positions and orientations of the AUT and probe were specified by a combination of rotations of the antenna's spectra and the *x*, *y*, *z* position of the probe used in the transmission equation. The simulation was carried out for rectangular Open Ended Waveguide (OEWG) probes using all of the higher order modes and also for the same probe where only the $\mu = \pm 1$ modes were used to calculate the probe patterns. Near-field simulations for the θ- and ϕ-polarised spherical near-fields can be found presented in Figure 1 and 2 respectively. Here, red contours are used to denote a probe with higher order modes, and back contours denote a probe with only $\mu = \pm 1$ modes.

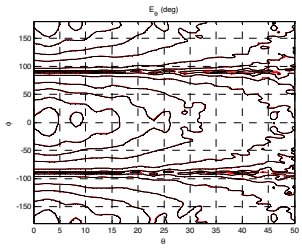

Figure 1. θ Polarized spherical near-field simulation.

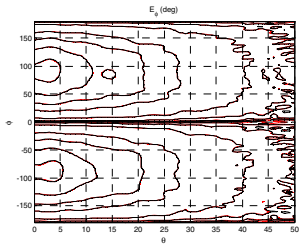

Figure 2. ϕ Polarized spherical near-field simulation.

As the agreement between the respective patterns was very good, the quantitative measure of similarity that was used to estimate the error in the measured spherical near-field and far-field data was the root-mean square (RMS) combination of the complex differences. This RMS combination represented the estimated error signal level relative to the peak amplitude. For both narrow beam array and SGH, the RMS ERR/SIG due to higher order modes of an OEWG was more than 35 dB below the peak of the main beam signal for all (θ, φ, a) positions tested. As complete spherical near-field simulations were produced, the effect on the far-field could also be determined as this data could be transformed using the standard spherical transformation. This is illustrated in Figure 3 which contains a comparison of the equivalent far-field patterns as obtained using a probe with higher order modes and one containing only $\mu = \pm 1$ modes.

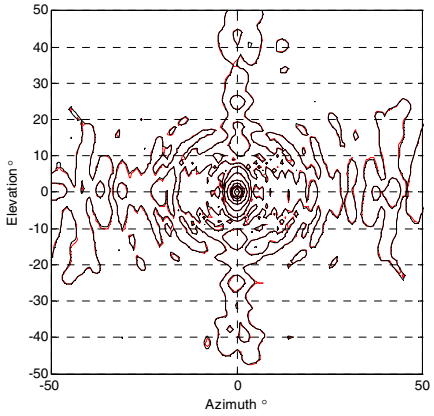

Figure 3. Equivalent far-field pattern, red is probe with higher order modes, black is probe with only mu = +/- 1 modes at a measurement radius of 1 MRE.

Again, the difference was determined and found to be primarily on the main beam and was 40 to 60 dB below main beam peak for measurement radii of 1 and 4 MRE respectively. Thus, the initial conclusion was that the effect of the higher order modes on typical measurements using OEWG probes would be smaller than other typical measurement errors and therefore have little practical effect on far-field results. The results of these simulations are presented and guidelines developed to aid in the choice of spherical near-field probes and measurement radii for typical antennas. Within this paper, these simulations are extended to obtain equivalent results for the case where a broadband dual ridge open boundary horn is used. Additionally this paper introduces a novel modification to the computationally intensive simulation technique that significantly reduces the amount of effort required in the calculation of the difference metrics.

II. PROBE AND AUT USED IN SIMULATION

Two similar probes were used in the simulation. They were dual ridged guide horns and one is shown in Figure 4. The RGP-10 horn operated over the band from 0.75 to 10.0 GHz and the RGP-20 over the band from 1.7 to 20 GHz and both were used at 9.4 GHz operating frequency of the AUT slotted array shown in Figure 5. This provided examples using both a high band and mid-band frequency for the probe.

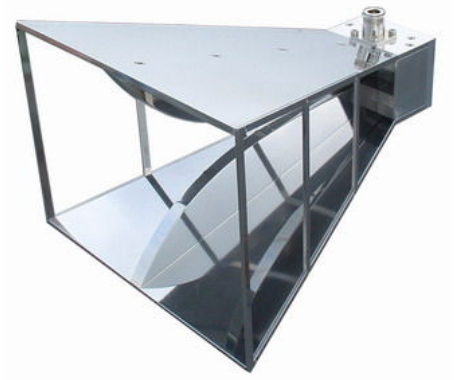

Figure 4 RGP10 ridged guide probe used in the simulation.

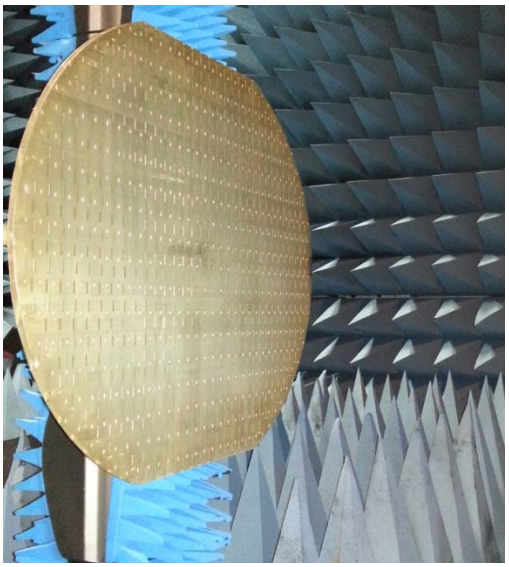

Figure 5 Slotted array used as the AUT in the simulations.

The probe patterns were measured on a spherical near-field range and the far-field patterns generated from these measurements were used to derive the plane-wave spectrum for the probes that was used in the simulation. These probes have a narrower beam than the Open Ended Waveguide Probes (OEWG) used in the previous simulations as illustrated in Figure 6. The measured probe data was also processed using the spherical near-field software and the

spherical mode coefficients were calculated and illustrated in Figure 7. These are the spherical mode amplitudes for the RGP20 probe for s = 1 and m ≥ 0 and illustrate that the higher order modes for |m| ≠ 1 are larger than those for the OEWG and should produce a greater effect when they are neglected in the spherical probe correction process. In particular, the m = 3 mode is nearly as large as the m = 1 mode. Using these probes provides one way to determine how large the higher mode amplitudes may be before causing significant errors in the spherical processing that assumes the probe has only first order modes.

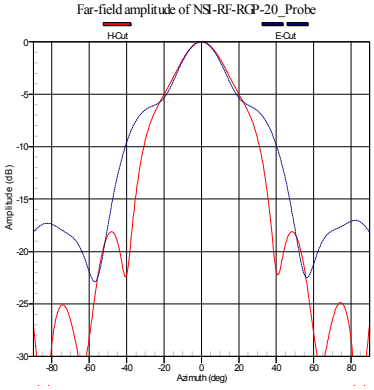

Figure 6 Principal plane patterns for the RGP-20 probe.

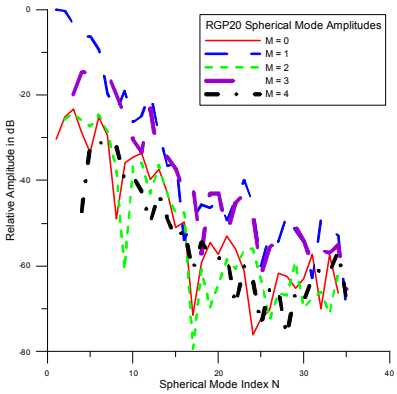

Figure 7 Amplitudes for spherical modes of the RGP20 probe

III. SIMULATION NUMERICAL PROCESSING USING THE CONCEPT OF A DIFFERENCE PROBE

The simulation uses the plane wave spectra for both the AUT and the probe and calculates the probe output for each (θ,ϕ) point on the measurement hemisphere by first rotating the AUT plane wave spectrum by the specified (θ,ϕ) angles and interpolating to a (k_x, k_y) grid. The plane wave spectrum of the probe is also rotated about the z-axis of the probe by the angles $\chi = 0$ *and* $\chi = 90$ to simulate the two probe rotations of a spherical near-field measurement. The plane wave transmission equation in (1) is then used to calculate the probe output at each point on the measurement sphere for the two probe rotation angles and this simulated near-field data can be transformed using the standard spherical software to produce the probe-corrected far-field of the AUT. In the previous study, this simulation for a given measurement distance was performed once using only the first order, μ=±1spherical modes for the probe and a second time using all the spherical modes. The difference in either the near-field or far-field results for the two probes was used as a measure of the error caused by neglecting the higher order modes.

$$b_0'(\theta,\phi,r,\chi) = F' a_0 \iint \vec{t}_{10}(\vec{K},\theta,\phi) \bullet \vec{s}_{02}'(\vec{K},\chi) e^{i\gamma r}\, dk_x dk_y$$

where

a_0 = Input amplitude and phase to AUT

$b_0'(\theta,\phi,z,\chi)$ = Probe output amplitude and phase for probe at x=0, y=0, z=r and rotated about the probe z-axis by the angle χ

$\vec{t}_{10}(\vec{K},\theta,\phi)$ = Rotated AUT plane-wave transmitting spectrum

$\vec{s}_{02}'(\vec{K},\chi)$ = Probe plane-wave receiving spectrum for χ rotation

(1)

A more efficient processing is realized and additional insight into the effect of the higher order modes is provided by modeling a general probe as the sum of an ideal probe with only the first order modes and a *difference* probe with only the higher order modes.

$$\vec{s}_{02}'(\vec{K},\chi) = \vec{s}_{02F}'(\vec{K},\chi) + \Delta_{02H}(\vec{K},\chi)$$

where

$\vec{s}_{02F}'(\vec{K},\chi)$ = Ideal first order probe using $\mu = \pm 1$ modes of actual probe.

$\Delta_{02H}(\vec{K},\chi)$ = Higher order probe using $\mu \neq \pm 1$ modes of actual probe.

(2)

The far-field pattern and therefore the receiving plane wave spectrum for the difference probe can be calculated by the spherical software using the measured probe near-field data and setting the first order modes to zero when the far-field is calculated. The error in the near-field data due to the higher order modes can be calculated directly in a single step by using only the difference probe spectrum in the transmission equation. The far-field error can then be calculated by processing this error near-field data using the standard spherical software.

Figures 8 -10 show the far-field pattern for the RGP20 probe using all the spherical modes, using only the first order modes and using only the non-first order modes. These represent the actual probe, the ideal first order probe and the difference probe respectively. The patterns for the difference probe and the ideal probe are normalized to the peak of the actual probe pattern so they represent the relative responses of

the three probes. Figure 10 clearly shows why the higher order modes have such a small effect on the measured near-field data and therefore the simulated AUT far-field pattern. The difference probe as defined by (2) has a deep null in its receiving pattern along the two principal planes and the lobes along the diagonal axes are 20 dB below the peak of the actual probe. In a spherical near-field measurement where the probe is pointed towards the center of the sphere for all (θ,ϕ) positions, the probe's response is determined by the portion of the probe pattern near the on-axis direction. For small measurement distances approaching the minimum sphere, the angular region will include the diagonal lobes and the integrated response will be larger than the depth of the null. But as the distance increases, the angular region of influence will decrease to a small region near-the on-axis null and the effect of the higher order modes will become very small. This is the trend that was demonstrated by the previous simulations for the OEWG probe and was repeated in the current results for the broad band probes.

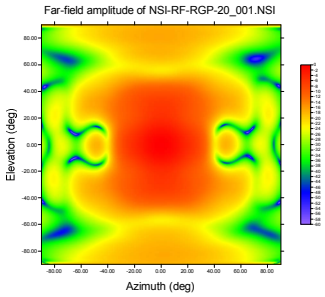

Figure 8 Far-field using all spherical modes

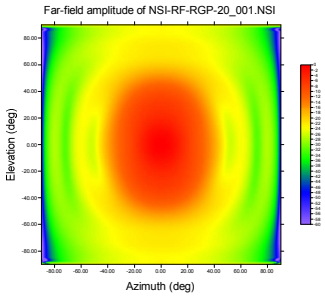

Figure 9 Far-field using only first order spherical modes

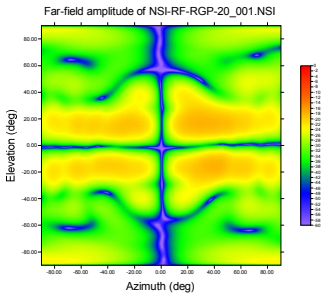

Figure 10 Far-field using non first order spherical modes

It may be possible to infer the magnitude of the difference probe's response as a function of measurement radius using only the pattern of the difference probe, however at present the full simulation using (1) and the pattern of the difference probe is used.

IV. SIMULATION RESULTS FOR THE BROADBAND HORN PROBES

The simulated results are presented in three different formats. In the first, the 2D near-field is computed using the difference probe on a (θ,ϕ) grid for a fixed measurement radius. An example is shown in Figure 11.

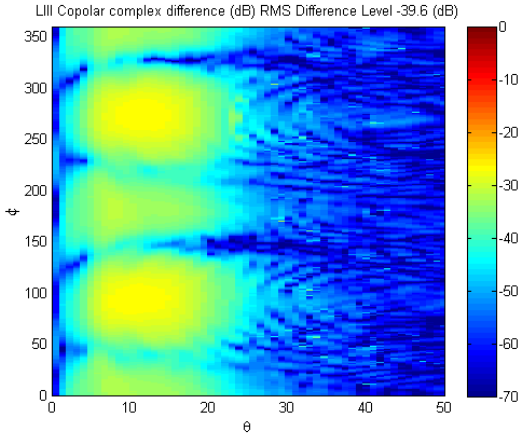

Figure 11 Simulated near-field amplitude for the difference probe for measurement radius of 2*MRE.

The far-field from this data is shown in Figure 12 and represents the error in the far-field pattern due to neglecting the higher order modes.

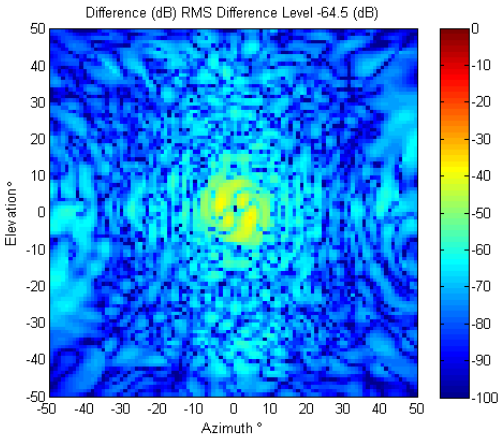

Figure 12 AUT far-field pattern for the difference probe computed with simulated near-field data for measurement radius of 2*MRE.

This process can be repeated for other measurement radii or the near-field error as a function of measurement radius can be computed for selected (θ,ϕ) points in the spherical grid to produce the near-field error versus distance shown in Figure 13.

From similar graphical results for different measurement parameters the magnitude and character of the near-field and far-field error due to neglecting the higher order modes in the processing can be determined. Guidelines for the use of broadband probes for spherical near-field measurements can then be established.

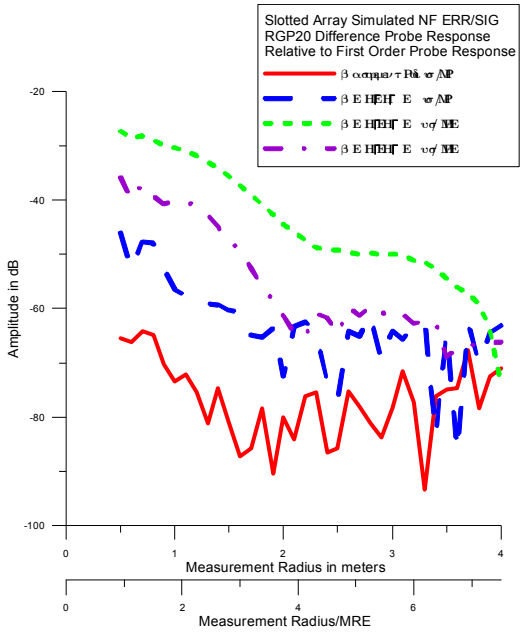

Figure 13 Near-field error due to neglecting higher order modes for selected near-field points.

V. SUMMARY OF RESULTS FOR THE BROADBAND PROBES

The results are similar to those for the OEWG probe. At the minimum measurement radius there are points in the near-field where the amplitude errors due to the higher order modes are only 30 dB below the correct values and this is high enough that it could be observed in an actual measurement. The effect on the far-field pattern is primarily on the main beam and the sidelobes have very small errors. The peak main beam errors are on the order of 40 dB below the main beam peak which may not be acceptable for high accuracy measurements. This level can be reduced by using measurement radii greater than 2*MRE and the graphical results can be used to determine the required distance for a desired accuracy level.

REFERENCES

[1] P.F. Wacker, "Near-field antenna measurements using a spherical scan: Efficient data reduction with probe correction", Conf. on Precision Electromagnetic Measurements, IEE Conf. Publ. No. 113, pp. 286-288, London, UK, 1974.

[2] F. Jensen, "On the probe compensation for near-field measurements on a sphere", Archiv für Elektronik und Übertragung-stechnik, Vol. 29, No. 7/8, pp. 305-308, 1975.

[3] J.E. Hansen, (Ed.) "Spherical near-field antenna measurements", Peter Peregrinus, Ltd., on behalf of IEE, London, 1988.

[4] T.A. Laitinen, S. Pivnenko, O. Breinbjerg, "Odd-order probe correction technique for spherical near-field antenna measurements," Radio Sci., vol. 40, no. 5, 2005.

[5] T.A. Laitinen, O. Breinbjerg, "A first/third-order probe correction technique for spherical near-field antenna measurements using three probe orientations," IEEE Trans. Antennas Propag., vol. 56, pp. 1259–1268, May 2008.

[6] T.A. Laitinen, J. M. Nielsen, S. Pivnenko, O. Breinbjerg, "On the application range of general high-order probe correction technique in spherical near-field antenna measurements," presented at the 2nd Eur. Conf. on Antennas and Propagation (EuCAP'07), Edinburgh, U.K. Nov. 2007.

[7] T.A. Laitinen, S. Pivnenko, O. Breinbjerg, "Theory and practice of the FFT/matrix inversion technique for probe-corrected spherical near-field antenna measurements with high-order probes", IEEE Trans. Antennas Propag., vol. 58,, No. 8, pp. 2623–2631, August 2010.

[8] T.A. Laitinen, S. Pivnenko, "On the truncation of the azimuthal mode spectrum of high-order probes in probe-corrected spherical near-field antenna measurements" AMTA, Denver, November 2012.

[9] A.C. Newell, S.F. Gregson, "Estimating the effect of higher order modes in spherical near-field probe correction", AMTA 34th Annual Meeting & Symposium, Seattle, WA, October. 2012.

[10] A.C. Newell, S.F. Gregson, "Higher Order Mode probes in Spherical Near-Field Measurements", EuCAP, Gothenburg, April, 2013.

[11] A.C. Newell, S.F. Gregson, "Estimating the Effect of Higher Order Modes in Spherical Near-Field Probe Correction", AMTA 35th Annual Meeting & Symposium, Seattle, WA, October. 2013.